Phase Diagram of the Triangular Extended Hubbard Model

Luca F. Tocchio,[1,2] Claudius Gros,[1] Xue-Feng Zhang (张学锋),[3] and Sebastian Eggert[3]
[1]Institute for Theoretical Physics, University of Frankfurt, Max-von-Laue-Straße 1, D-60438 Frankfurt, Germany
[2]CNR-IOM-Democritos National Simulation Centre and International School for Advanced Studies (SISSA), Via Bonomea 265, I-34136 Trieste, Italy
[3]Physics Department and Research Center OPTIMAS, University of Kaiserslautern, D-67663 Kaiserslautern, Germany
(Received 13 February 2014; published 12 December 2014)

We study the extended Hubbard model on the triangular lattice as a function of filling and interaction strength. The complex interplay of kinetic frustration and strong interactions on the triangular lattice leads to exotic phases where long-range charge order, antiferromagnetic order, and metallic conductivity can coexist. Variational Monte Carlo simulations show that three kinds of ordered metallic states are stable as a function of nearest neighbor interaction and filling. The coexistence of conductivity and order is explained by a separation into two functional classes of particles: part of them contributes to the stable order, while the other part forms a partially filled band on the remaining substructure. The relation to charge ordering in charge transfer salts is discussed.

DOI: 10.1103/PhysRevLett.113.246405 PACS numbers: 71.10.Fd, 71.27.+a, 75.25.Dk

The study of frustrated and strongly interacting systems in two dimensions has received an unbroken intensity of research activities in recent years. Just to name a few examples, spin-liquid and topological states have been postulated in frustrated two-dimensional antiferromagnets [1–5], supersolid phases have been established for hard-core bosons on a triangular lattice [6–8], and the concept of deconfined quantum critical points [9] has sparked a tremendous interest in the search of exotic phase transitions.

Above examples involve essentially spinlike systems, where charge degrees of freedom only play a passive role. When both spin and charge degrees of freedom are considered at incommensurate filling the situation potentially becomes even more interesting. In this context organic conductors have become an interesting field of research. In particular, in the charge transfer salts θ-$(\mathrm{BEDT\text{-}TTF})_2X$ [10–17] the molecules are arranged on an anisotropic triangular lattice with incommensurate filling, so this material class shows interesting frustration effects. Conductors on frustrated lattices are also relevant in the context of superconductivity as, for example, in the layered triangular compound $\mathrm{Na}_x\mathrm{CoO}_2$ [18–20] where interesting textures have been predicted recently [21,22].

For the description of the spin and charge degrees of freedom in these compounds it is natural to use the extended Hubbard model on the triangular lattice

$$\mathcal{H} = -t\sum_{\langle i,j\rangle,\sigma} c^{\dagger}_{i,\sigma}c_{j,\sigma} + \mathrm{H.c.} + U\sum_{i} n_{i,\uparrow}n_{i,\downarrow} + V\sum_{\langle i,j\rangle} n_i n_j, \tag{1}$$

where we have used standard notation. In addition to the relevance for the systems mentioned above, this prototypical model is also of fundamental interest in order to understand the interplay of frustration and strong interactions with spin and charge degrees of freedom at arbitrary filling $n = \langle n_\uparrow + n_\downarrow \rangle$. Unfortunately, analytical and numerical studies of this system are far from trivial and to our knowledge it has not yet been analyzed with quantum many body simulations for incommensurate filling. In this Letter we now use numerical variational Monte Carlo simulations in order to establish the phase diagram as a function of filling and interaction strength. In addition to the ordinary metallic phase, three interesting phases are found, where long-range charge order and metallic conductivity are present simultaneously as depicted in Fig. 1, which summarizes most of our findings.

The commensurate one-third filled case ($n = 2/3$) has been discussed in Ref. [16]. Quite intuitively, for strong $V \gtrsim U/3 \gg t$ any nearest neighbor occupation is forbidden, resulting in an insulating ordered phase with exactly two electrons on one sublattice (200 order), while for weaker nearest neighbor repulsion double occupancy is forbidden and instead two sublattices are half-filled in a hexagonal order (110 order); see Fig. 1. A spin-liquid phase is excluded, due to the breaking of the translational invariance in the insulating region.

For incommensurate filling, the 110 phase in Fig. 1 represents a state where one of the three triangular sublattices remains empty and all the electrons occupy the other two sublattices in a hexagonal density pattern in order to minimize the nearest neighbor repulsion. Since the hexagonal order necessarily contains holes for $n < 2/3$, this phase becomes conducting. Interestingly, this coexistence of two counterintuitive properties (order and conductivity) is directly related to the supersolid state on triangular lattices which has been established for hardcore bosons

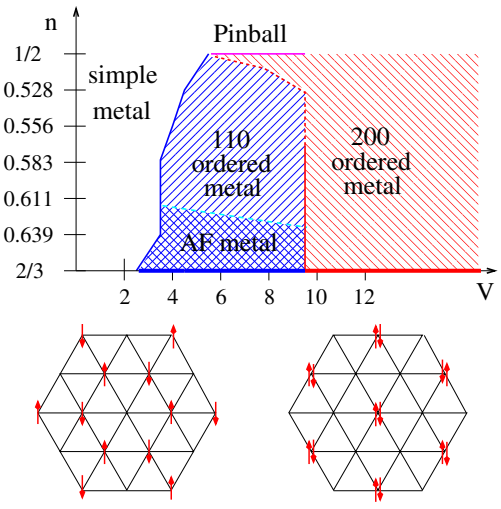

FIG. 1 (color online). Upper panel: Phase diagram of the Hubbard model for $U = 30t$ as a function of V/t and filling. Three phases can be identified: a simple metal, a metallic state with a 110 charge order, and a metallic state with a 200 charge order. The charge order regions are insulating at commensurate filling $n = 2/3$ (thick lines) and metallic otherwise. In the limiting case $n = 1/2$ the 200 charge ordered phase is preempted by the pinball one. For filling $0.62 \lesssim n \leq 2/3$ we find an indication for magnetic order (AF) within the 110 charge ordered metal. Lower panel: sketch of the 110 charge order (left) and of the 200 charge order (right).

[6–8], and has analogously been postulated for spinless fermions [23,24]. Simulations for hardcore bosons have shown that a separation into two types of holelike particles is possible [25]: One part creates the ordered state by keeping one sublattice empty, while the other part can move freely on the hexagonal structure (partial liquid). However, as the filling approaches $n = 2/3$ we observe a transition to a phase where antiferromagnetic (AF) order coexists with conductivity, which requires a different mechanism as described below.

For the extended Hubbard model we find a third interesting phase in the form of a 200 order in Fig. 1: Double occupancy occurs only on one sublattice which is reduced with filling and gives an ordered state. This state has some surprising properties, since the observed conductivity implies that the other two sublattices are not completely empty either. The occupation on those two sublattices therefore *increases* with decreasing filling, which leads to conductive behavior. The phase transition between the 110 and 200 states is first order close to commensurate filling but may become second order for $n \lesssim 0.57$. For large hoppings a transition to a simple metal occurs.

In the quarter-filled $n = 1/2$ case, the 200 ordered metal is preempted by a region that has been named the "pinball phase" in Refs. [23,24]. Also this phase is characterized by increased occupation on one sublattice and the depletion of the other two; however, in the pinball phase the number of double occupancies is small and there is still a large fraction of electrons residing on the two sublattices with reduced occupation.

In order to simulate the model in Eq. (1) at zero temperature we have used the variational Monte Carlo method [26], which gives very good results [27] even for correlated and frustrated systems by numerically sampling expectation values over a variational ansatz. A powerful correlated variational state is given by [28–31] $|\Psi_{\mathrm{FS}}\rangle = \mathcal{J}|\mathrm{FS}\rangle$, where $|\mathrm{FS}\rangle$ is the noninteracting filled Fermi sea, to which a finite small superconductive term is added in order to regularize the wave function, i.e., to separate the highest occupied and the lowest unoccupied states by a gap. The term $\mathcal{J} = \exp(-1/2\sum_{ij} v_{ij} n_i n_j)$ is a density-density Jastrow factor, where the v_{ij}'s are optimized with variational Monte Carlo calculations for every independent distance $|i - j|$ (including on site).

Backflow correlations further improve the correlated state $|\Psi_{\mathrm{FS}}\rangle$; in this approach, each orbital that defines the unprojected state $|\mathrm{FS}\rangle$ is taken to depend upon the many-body configuration in order to incorporate virtual hopping processes [32]. The excellent accuracy of the variational estimate is shown in the Supplemental Material [33]. The non-interacting state $|\mathrm{FS}\rangle$ also includes three different chemical potentials as variational parameters, one for each sublattice. We must emphasize, however, that even for a uniform variational chemical potential the charge ordered metallic states spontaneously appears in the phase diagram at arbitrary filling [33], which demonstrates the stability of this phenomenon.

Finally, a coupling to an external field can be added in order to check if the ground state is magnetically ordered. All results presented here are obtained by fully incorporating the backflow corrections and optimizing individually [36] every variational parameter in the wave function. We then perform a Monte Carlo sampling of the observables. The error bars are always smaller than the symbol size and their order of magnitude is provided in the figure captions.

The static structure factor $N(q) = \langle n_{-q} n_q \rangle$ is a good indicator for metallic behavior, where $n_q = 1/\sqrt{L}\sum_{r,\sigma} e^{iqr} n_{r,\sigma}$ is the Fourier transform of the particle density. The metallic phase is characterized by $N(q) \propto q$ for $q \to 0$, which implies a vanishing gap for particle-hole excitations. On the contrary, $N(q) \propto q^2$ for $q \to 0$, implies a finite charge gap and insulating behavior [32]. These relations hold also with respect to the variationally optimized ground state, as shown in the Supplemental Material [33].

We find conducting behavior everywhere except for $n = 2/3$ and $V/t \gtrsim 3$, as shown in Fig. 2. Interestingly, a diverging behavior of $N(q \to 0)$ is observed in the 200 phase, which we attribute to a q^2 dispersion relation at effective low filling as explained below.

In order to distinguish between the different kinds of charge ordering in the model, we plot in Fig. 3 the

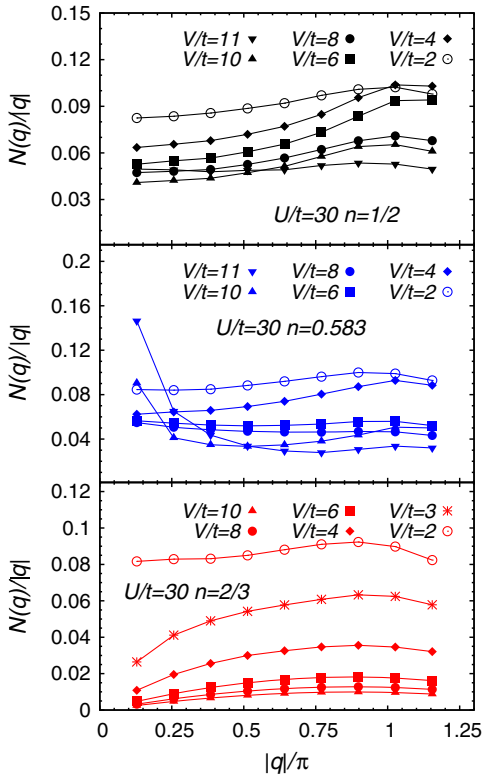

FIG. 2 (color online). $N(q)/q$ as a function of $|q|/\pi$ for different values of V/t. Data are shown along the line between $\Gamma = (0,0)$ and $\mathbf{M} = (0, 2\pi/\sqrt{3})$ in the Brillouin zone for three different values of doping $n = 1/2$, $n = 0.583$, and $n = 2/3$ from above at system size $L = 342$. The absolute error bars on $N(q)$ are always smaller than 10^{-3} for all the shown q points.

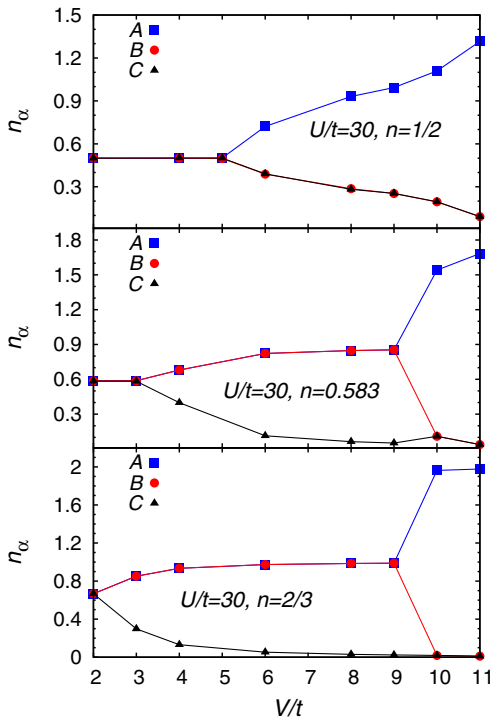

FIG. 3 (color online). Electronic density n_α in each of the three sublattices A, B, and C as a function of V/t. Data are presented for the three values of the total electronic density $n = 1/2$, $n = 0.583$, and $n = 2/3$. The on-site Coulomb repulsion is $U = 30t$ and the lattice size is $L = 324$. The absolute error bars on the densities range from 5×10^{-4} to 5×10^{-5}.

electronic density per sublattice n_α with $\alpha = A, B, C$ on each of the three sublattices. Within the non-ordered metallic phase, the electronic density is uniform, while in the 110 region one sublattice depletes, with the electrons forming an hexagonal density order; see Fig. 1. Finally, in the 200 phase one sublattice is occupied with a substantial density and an increasing double occupancy.

Both the cases $n = 2/3$ and $n = 0.583$ in Fig. 3 show a clear distinction between the three regimes, while in the limiting case $n = 1/2$ we observe a single sublattice being more and more occupied as long as the ratio V/t increases. For $V/t \approx 10$ a rapid crossover is observed for $n = 1/2$, separating the pinball phase from the 200 ordered metal regime [33], with an associated rapid increase in double occupancy.

Even though a high density of electrons on one sublattice is the expected behavior for a small hopping t and $3V > U$, the 200 ordered metal has rather unusual properties. First of all it is far from obvious why this ordered state is conducting. In the 110 order the conductivity can be explained by mobile holes moving on a hexagonal substructure [23–25]. In the 200 order on the other hand, holes only appear on one sublattice which is not connected, so this argument fails. Moreover, we have checked that all the electrons that are in a doubly occupied state also contribute to the ordering, so conduction by virtual hopping or by pair hopping can be ruled out. We present in Fig. 4 (left) the charge order parameter ϕ as defined by

$$\phi = \lim_{|i-j|\to\infty} \langle (n_{i,\uparrow} n_{i,\downarrow})(n_{j,\uparrow} n_{j,\downarrow}) \rangle, \tag{2}$$

where the distance $|i - j|$ connects points on the same sublattice, and compare it with the density of double occupancies $D = \langle n_\uparrow n_\downarrow \rangle$. If the relation $\phi = 3D^2$ holds, all the double occupancies participate to the charge order, otherwise, if $\phi < 3D^2$, a fraction of the double occupancies is mobile outside the 200 pattern, with the limiting case $\phi = D^2$ corresponding to a uniform distribution of double occupancies in the lattice. According to the result shown in Fig. 4 (left) for $V/t = 10$, the relation $\phi = 3D^2$ is verified in all the doping range and the system separates into charge ordered double occupancies and free electrons that are responsible for the conduction mechanism. Therefore, conductivity appears to require a small density of electrons on the two sublattices which are empty for $n = 2/3$; i.e., the density on the two almost empty sublattices must increase with decreasing n. In Fig. 4 (right) we show δn, that represents the electronic filling on the hexagonal substructure, which is available for a conducting band in

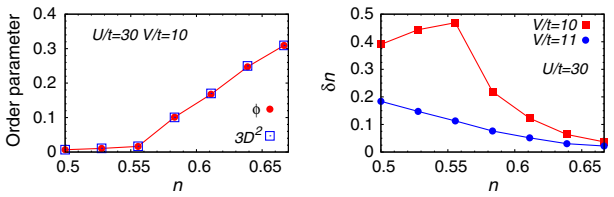

FIG. 4 (color online). Left: Charge order parameter ϕ, see Eq. (2), and $3D^2$, where D is the density of double occupancies, as a function of the electronic density n. Right: Filling of the hexagonal substructure δn as a function of the total electronic density n within the 200 region of the phase diagram, at $V/t = 10$ and $V/t = 11$. Data are shown at $U = 30t$ and size $L = 324$. The absolute error bars on the order parameter ϕ and on $3D^2$ are always smaller than 10^{-4}.

the 200 regime. In the case $V/t = 11$ it is clear that δn increases at increasing doping, while in the case $V/t = 10$ there is a small decrease in δn when doping becomes large, i.e., $n \lesssim 0.57$. This is just a consequence of the small and almost constant number of double occupancies that occurs at $V/t = 10$ in the range $1/2 \leq n \lesssim 0.57$; see Fig. 4 (left). Indeed, in this density range the transition between the 110 and the 200 phases becomes second order with a smooth increase of the number of double occupancies as a function of V/t. The effective filling of electrons on the hexagonal substructure δn is rather low in the range $0.57 \lesssim n \leq 2/3$. Accordingly, the electrons follow a q^2 dispersion relation at the bottom of the band, which explains the divergence of $N(q \to 0)$ in this phase, as discussed above in Fig. 2.

Finally, we also tested for magnetic order and found that an antiferromagnetic state has lower variational energy for fillings $0.62 \lesssim n \leq 2/3$ as indicated in Fig. 1. While antiferromagnetic order is expected for commensurate insulating fillings, it should immediately be destroyed by moving holes on the hexagonal substructure. However, for very small doping close to filling $2/3$ the energy gain from hopping of order $t(2/3 - n)$ is not sufficient to overcome the energy gain from long-range antiferromagnetism of order nt^2/U. Nonetheless, second order hopping processes of holes via the depleted sites are still possible without changing the spin orientation, so that a finite conductivity is observed in coexistence with antiferromagnetic order in this special case. This phase is stabilized for a large second order hopping amplitude t^2/V in agreement with our finding in Fig. 1.

In conclusion, we have analyzed the extended Hubbard model on the triangular lattice as a function of interaction strength and filling. The phase diagram in Fig. 1 shows three ordered metallic phases at incommensurate filling. A simple metallic phase is confirmed for large hopping. With increasing interaction strength an ordered metal with a 110-type order is observed, due to the appearance of holes on a stable hexagonal order, which is analogous to the underlying mechanism for supersolidity [25]. For filling close to $2/3$ we observe a phase transition to an antiferromagnetically ordered metal. A 200-ordered phase with one double occupied sublattice is found for still larger nearest neighbor repulsion, which surprisingly also shows conductive behavior. The observed occupancy of the sublattices B and C and the electronic properties are consistent with a band on the hexagonal substructure with very low filling. This is surprising, since the strong nearest neighbor repulsion naively presents a large energy barrier for electrons on the hexagonal substructure next to the double occupied sites. The detailed mechanisms of the conductive behavior both in the 200 phase and in the 110 antiferromagnetic phase remain a topic of future research.

Experimentally, charge ordering phenomena in charge transfer salts have been researched with a large variety of methods, e.g., NMR, x-ray, and infrared or Raman spectroscopy [37]. Coexistence of metallic behavior and charge ordering has only been observed in few cases for θ-$(\mathrm{BEDT\text{-}TTF})_2X$ and β''-$(\mathrm{BEDT\text{-}TTF})(\mathrm{TCNQ})$ charge transfer salts and only for short range charge order [38]. The scenario we have proposed in this Letter predicts a coexistence of metallic behavior and long-range order, which is not due to a partial instability of the Fermi surface. Instead, we can identify a separation into two functional classes of particles (or holes): part of them contribute to a stable order on one sublattice, while another part forms a partially filled band on the remaining hexagonal substructure.

We would like to thank the Deutsche Forschungsgemeinschaft for financial support through the collaborative research centre SFB/TR49 and Federico Becca for useful discussions. L. F. T. is thankful for partial support from the Ministero dell'Istruzione, dell'Universita e della Ricerca through Grant No. A.AC.FISI.774 PRIN 2010-2011.

[1] L. Balents, Nature (London) **464**, 199 (2010).
[2] S. Yan, D. Huse, and S. White, Science **332**, 1173 (2011).
[3] L. F. Tocchio, H. Feldner, F. Becca, R. Valentí, and C. Gros, Phys. Rev. B **87**, 035143 (2013).
[4] Y. Iqbal, F. Becca, S. Sorella, and D. Poilblanc, Phys. Rev. B **87**, 060405 (2013).
[5] X.-F. Zhang and S. Eggert, Phys. Rev. Lett. **111**, 147201 (2013).
[6] S. Wessel and M. Troyer, Phys. Rev. Lett. **95**, 127205 (2005).
[7] R. G. Melko, A. Paramekanti, A. A. Burkov, A. Vishwanath, D. N. Sheng, and L. Balents, Phys. Rev. Lett. **95**, 127207 (2005).
[8] D. Heidarian and K. Damle, Phys. Rev. Lett. **95**, 127206 (2005).
[9] T. Senthil, A. Vishwanath, L. Balents, S. Sachdev, and M. P. A. Fisher, Science **303**, 1490 (2004).
[10] C. Hotta, J. Phys. Soc. Jpn. **72**, 840 (2003).
[11] M. Udagawa and Y. Motome, Phys. Rev. Lett. **98**, 206405 (2007).
[12] L. Cano-Cortés, A. Ralko, C. Février, J. Merino, and S. Fratini, Phys. Rev. B **84**, 155115 (2011).

[13] J. Merino, A. Ralko, and S. Fratini, Phys. Rev. Lett. **111**, 126403 (2013).
[14] T. Mori, J. Phys. Soc. Jpn. **72**, 1469 (2003).
[15] H. Watanabe and M. Ogata, J. Phys. Soc. Jpn. **75**, 063702 (2006).
[16] H. Watanabe and M. Ogata, J. Phys. Soc. Jpn. **74**, 2901 (2005).
[17] J. Merino, Phys. Rev. Lett. **99**, 036404 (2007).
[18] K. Takada, H. Sakurai, E. Takayama-Muromachi, F. Izumi, R. A. Dilanian, and T. Sasaki, Nature (London) **422**, 53 (2003).
[19] C. Honerkamp, Phys. Rev. B **68**, 104510 (2003).
[20] M. L. Kiesel, C. Platt, W. Hanke, and R. Thomale, Phys. Rev. Lett. **111**, 097001 (2013).
[21] K. Jiang, S. Zhou, and Z. Wang, Phys. Rev. B **90**, 165135 (2014).
[22] S. Zhou and Z. Wang, Phys. Rev. Lett. **98**, 226402 (2007).
[23] C. Hotta and N. Furukawa, Phys. Rev. B **74**, 193107 (2006).
[24] C. Hotta and N. Furukawa, J. Phys. Condens. Matter **19**, 145242 (2007).
[25] X.-F. Zhang, R. Dillenschneider, Y. Yu, and S. Eggert, Phys. Rev. B **84**, 174515 (2011).
[26] D. Ceperley, G. V. Chester, and M. H. Kalos, Phys. Rev. B **16**, 3081 (1977).
[27] R. Kaneko, S. Morita, and M. Imada, J. Phys. Conf. Ser. **454**, 012046 (2013).
[28] C. Gros, Phys. Rev. B **38**, 931(R) (1988).
[29] F. C. Zhang, C. Gros, T. M. Rice, and H. Shiba, Supercond. Sci. Technol. **1**, 36 (1988).
[30] C. Gros, Ann. Phys. (N.Y.) **189**, 53 (1989).
[31] M. Capello, F. Becca, M. Fabrizio, S. Sorella, and E. Tosatti, Phys. Rev. Lett. **94**, 026406 (2005).
[32] L. F. Tocchio, F. Becca, and C. Gros, Phys. Rev. B **83**, 195138 (2011).
[33] See Supplemental Material at http://link.aps.org/supplemental/10.1103/PhysRevLett.113.246405 for the accuracy of the variational ansatz, the uniform variational wave function, the momentum dependence of $N(q)$ in the full Brillouin zone, the derivation of the formula for the charge gap when the true ground state is replaced by a variational approximation of it, and more details on the limiting $n = 1/2$ case. Included therein are Refs. [34,35].
[34] L. F. Tocchio, A. Parola, C. Gros, and F. Becca, Phys. Rev. B **80**, 064419 (2009).
[35] L. F. Tocchio, F. Becca, A. Parola, and S. Sorella, Phys. Rev. B **78**, 041101(R) (2008).
[36] S. Yunoki and S. Sorella, Phys. Rev. B **74**, 014408 (2006).
[37] For a review see, T. Takahashi, Y. Nogami, and K. Yakushi, J. Phys. Soc. Jpn. **75**, 051008 (2006).
[38] For a review see, K. Yakushi, Crystals **2**, 1291 (2012).